A SURVEY OF EARLY-TYPE STARS BASED ON THE TWO MICRON ALL SKY SURVEY DATABASE[1]

R. Ortiz
Escola de Artes, Ciências e Humanidades, Universidade de São Paulo, Avenida Arlindo Bettio 1000,
03828-000 São Paulo, SP, Brazil; ortiz@astro.iag.usp.br

M. Malacarne
Departamento de Física, Universidade Federal do Espírito Santo, Avenida Fernando Ferrari 514, 29060-900 Vitória, ES, Brazil

R. Wilhelm
Department of Physics, Texas Tech University, Campus Box 41051, Lubbock, TX 79409, USA

R. D. D. Costa, S. Rossi, and W. J. Maciel
Departamento de Astronomia, Instituto de Astronomia, Geofísica e Ciências Atmosféricas, Universidade de São Paulo,
Rua do Matão 1226, Cidade Universitária, 05508-900 São Paulo, SP, Brazil

and

A. F. M. Costa
Instituto de Física, Universidade Federal do Rio Grande do Sul, 91501-900 Porto Alegre, RS, Brazil
Received 2007 March 13; accepted 2007 June 11

ABSTRACT

We report the results of a spectroscopic survey of blue stars near the south Galactic pole, selected according to their color indices in the 2MASS database. The main scope of this work is to determine the nature of the objects that comprise the sample. Some characteristics of the Hβ, Hγ, and Hδ lines which are sensitive to temperature and gravity were measured and eventually compared with a grid of model atmospheres to obtain $T_{\rm eff}$ and log g. In some cases the data allowed a unique, reliable classification of the star. Among the 44 stars studied, 5 objects are reliably classified as subdwarfs, 12 as A-type stars, and 3 as field horizontal-branch (FHB) stars. The remaining objects are either A or FHB stars, but additional observations are necessary to distinguish between these two types. Neither degenerate nor low-gravity stars (post-AGB) have been identified in the sample.

Key words: Galaxy: halo — Galaxy: stellar content — stars: early-type — stars: horizontal-branch — subdwarfs — surveys

1. INTRODUCTION

The Galactic poles have long been explored in the quest for halo objects, especially field horizontal-branch (FHB) stars, including RR Lyrae variable stars. Because the absolute magnitudes of HB stars are in a narrow range (Gratton 1998), they can be used as standard candles to figure out the spatial distribution of stars in the halo (Sluis & Arnold 1998). Numerous surveys have been carried out to identify halo members, which can be gathered into two main groups: the photometric surveys, which make use of Strömgren and/or broadband photometry (Green et al. 1986; Noguchi et al. 1980; Stobie et al. 1987; Kilkenny et al. 1991), and the objective-prism surveys, which classify stars based on very low resolution spectra (Sanduleak & Pesch 1987; Sanduleak 1988). More recently, the completion of major CCD and infrared surveys has opened a new perspective in identifying blue stars in deep fields. The Sloan Digital Sky Survey, for example (York et al. 2000), covered a quarter of the sky in five colors. It has been used to identify white dwarfs (Harris et al. 2003) and blue horizontal-branch (BHB) stars at distances from 7 to 60 kpc from the Sun (Sirko et al. 2004). This lower limit of distance of BHB stars is caused by the saturation magnitude of the Sloan survey at $g = 15.5$. The infrared surveys DENIS and the Two Micron All Sky Survey (2MASS) constitute another important database to identify hot, bright stars far from the Galactic plane.

Ortiz (2002) and Brown et al. (2003, 2004), among others, have identified BHB stars, young stars, and other kinds of "blue" objects in these infrared surveys.

The discovery of main-sequence (MS) stars of early spectral type far from the Galactic plane is perhaps more remarkable than the identification of BHB stars. A few hundred MS stars of spectral types A and B have been identified so far (Conlon et al. 1990; Mitchell et al. 1998; Pier 1982, 1983), but it is not clear whether they have been ejected from the Galactic plane by collisions (Conlon et al. 1990) or whether they were formed in the halo itself (Conlon et al. 1992). Spectroscopic surveys can function as an effective tool to find more objects of this kind.

Unfortunately, the usage of color indices to classify stars is not very reliable. For instance, A and B MS stars show broadband color indices very similar to those of BHB stars. Brown et al. (2004) claim that BHB stars constitute only half the stars selected according to their infrared color indices. As an alternative, Strömgren photometry can be used more reliably (Stetson 1991; Flynn et al. 1994). Another good method is to measure the equivalent width of the Balmer lines, especially Hδ. The $D_{0.2}$ method (Pier 1983; Sommer-Larsen & Christensen 1986; Wilhelm et al. 1999a) also allows fine discrimination among the several kinds of blue stars, although the separation between BHB and MS stars remains unclear in many cases (Beers et al. 1992; Sirko et al. 2004). At stellar temperatures $T_{\rm eff} > 10,000$ K it becomes extremely difficult to separate BHB and MS stars, because the surface gravity of BHB stars increases to MS gravities in this regime. The high-resolution work by Behr (2003) on BHB stars in various globular

clusters illustrates this effect. In Figure 9 of that paper the extended HB of various clusters quickly approaches log g values typical of MS stars (log $g \simeq 4.0$). These data are also consistent with the theoretical zero-age HB by Dorman et al. (1993), which predicts a similar increase in log g. Therefore, it becomes nearly impossible for stars hotter than 10,000 K to separate the BHB from the MS using surface gravity as an indicator.

In this work we present the results of an infrared, flux-limited spectroscopic survey of the south Galactic cap, based on the 2MASS point-source catalog. The survey is especially aimed at stars that have been overlooked in previous surveys of this kind. Stars are classified according to their visual spectra, and some of their atmospheric parameters are determined. In § 2 the criteria used to select the sample are described; § 3 describes the observations; § 4 is devoted to presenting our results, including a summary of the techniques used to determine the nature of the stars; and our conclusions are presented in § 5.

2. THE SAMPLE

2.1. JHK Colors As a Tool to Select Early-Type Stars

The 2MASS (Skrutskie et al. 1997) covered the whole sky at three wavelengths, J ($\lambda = 1.25$ μm), H ($\lambda = 1.65$ μm), and K ($\lambda = 2.15$ μm), and is claimed to be complete up to magnitudes of 15.8, 15.1, and 14.3, respectively. The point-source catalog constitutes a fairly uniform photometric database, since each hemisphere was fully observed with the same set of telescopes, filters, and detectors. In this work we use the 2MASS catalog to select sources showing color temperatures greater than 10,000 K. Figure 1 shows a sample consisting of about 12,500 stars near the south Galactic pole together with intrinsic color indices of dwarfs calculated by Bessell & Brett (1988). The density of points does not represent the statistical distribution of colors, but it emphasizes the points near the lower left corner of the figure. These diagrams show that the MS runs almost perpendicular to the $H - K$ axis. Therefore, this color index is not very reliable for distinguishing stars by their temperature. On the other hand, both the $J - K$ and $J - H$ color indices show more explicit dependence on T. We are aware that, whatever the infrared color indices used, they do not constitute an accurate method to determine the temperature, because the spectral energy distribution approaches the Rayleigh-Jeans regime in the near-infrared. Nevertheless, this tool allows a rough selection of hot stars in large databases such as 2MASS, and the temperature can eventually be estimated based on spectral features of the observed stars.

2.2. Criteria for Selecting Early-Type Stars Near the South Galactic Pole with Good-Quality 2MASS Photometry

Once the $J - K$ and $J - H$ color indices have been chosen to select infrared sources according to their color temperature, additional selection criteria had to be adopted in order to select only sources that have good photometric measurements. A summary of the criteria used in this work is as follows:

1. $b < -60°$,
2. $J - H \leq 0.0$ and $J - K \leq 0.0$,
3. $J \leq 15.8$, $H \leq 15.1$, and $K_{\mathrm{short}} \leq 14.3$,
4. ph_qual flag $\neq$ X, U, F, E in the three bands.

The limitation in magnitude aims to select only sources within the completeness limit of the survey, as well as to avoid sources which would require too long an integration time when observed with a small telescope. The flags that accompany the magnitudes in the 2MASS catalog give information about problems that might have occurred during the measurements or the data reduction. The
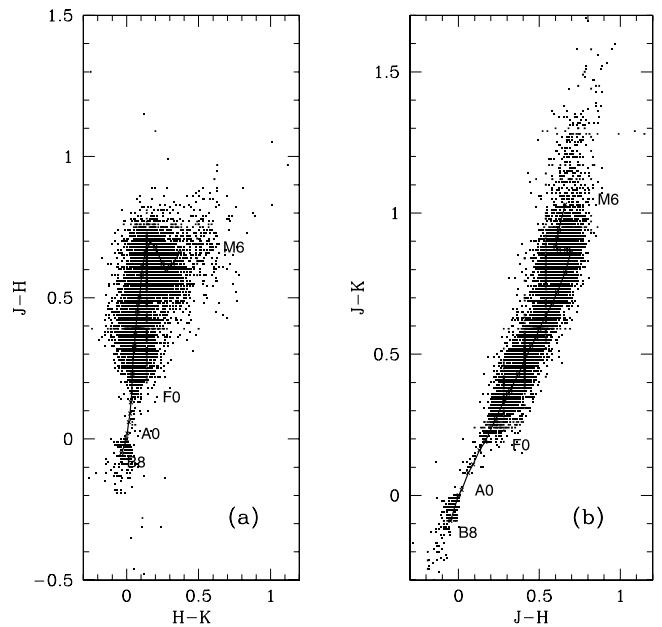

Fig. 1.—The 2MASS sources near the Galactic pole. The symbols represent sources with good photometry, according to the flags of the 2MASS point-source catalog. The solid line represents the standardized colors of MS stars according to Bessell & Brett (1988), identified by their spectral types along the curve. The density of points does not represent the statistical distribution in color, but it was made to emphasize the population of objects with $J - H < 0$, $H - K < 0$, and $J - K < 0$.

rejection of sources with bad ph_qual flags aimed to exclude stars which had problems with their photometry during the data reduction. The meaning of the flags noted above is as follows: X indicates that there is a detection, but no useful brightness estimate can be extracted using any algorithm; U indicates an upper limit on the magnitude; F designates either aperture photometry or a saturated source; and E indicates that either the quality of the profile-fit photometry is very poor or the profile-fit photometry does not converge, and an aperture magnitude is reported. On the other hand, sources with flags B and C have been included because their fluxes are reliable, although with smaller signal-to-noise ratios (S/N = 7 and 5, respectively). According to the 2MASS Survey Strategy Requirements, version 1.7 (Cutri et al. 2003), the restrictions of the limiting magnitudes of the three bands above correspond to S/N $\geq$ 10. However, a few cases of sources showing photometric flags B, C, and D have been noted; thus, the values concerning the S/Ns must be considered approximate.

Despite all the precautions taken in the 2MASS reduction pipeline, a few problems persist with the photometry. About 20% of the sources selected according to the criteria specified above are in fact optical pairs or binaries. Although the bl_flag of these sources indicates that the components are not blended and the photometric method used was profile fitting, their JHK color indices are incompatible with the spectral type of the stars. A search in the SIMBAD database shows that their spectral types are generally F or later. In order to avoid such objects, all sources which appear double in the Digitized Sky Survey were removed from the observation list.

The JHK error bars are the main source of error in the determination of spectral type. On average, they are 0.03, 0.05, and 0.07 mag in the J, H, and K bands, respectively, for magnitudes greater than 14.0, which is near the limit considered for the K band. Consequently, the errors in the color indices are $\sigma(J - H) = 0.06$ and $\sigma(J - K) = 0.08$ mag, which represent five spectral subclasses for both indices. This means that even stars of A5 spectral type may show $(J - H)$ and $(J - K)$ near zero and may be

TABLE 1
2MASS Data of the Sample Observed during This Survey

Number (1)	2MASS Name (2)	l (3)	b (4)	Blue Mag. (5)	Red Mag. (6)	J (7)	σ_J (8)	H (9)	σ_H (10)	K (11)	σ_K (12)	$B-V$ (13)
1..................	22361663−3142130	15.861	−60.332	12.70	13.80	13.834	0.029	14.021	0.047	14.059	0.055	−0.2
2..................	22385421−2352209	31.670	−60.003	11.57	11.94	12.180	0.024	12.254	0.025	12.297	0.023	−0.07
3..................	22393762−2455025	29.689	−60.389	12.50	12.80	12.708	0.023	12.721	0.022	12.788	0.025	−0.21
4..................	22475352−3829408	1.278	−61.836	14.10	16.30	13.902	0.032	13.921	0.044	13.969	0.063	. . .
5..................	22480188−3503104	8.503	−62.543	12.33	12.29	12.770	0.024	12.825	0.025	12.842	0.030	. . .
6..................	22501122−3759588	2.064	−62.396	13.90	14.20	14.050	0.029	14.071	0.040	14.087	0.069	. . .
7..................	22515349−4355577	350.090	−60.699	12.80	14.30	13.569	0.027	13.595	0.022	13.645	0.049	. . .
8..................	22524524−2147476	37.585	−62.539	12.10	12.37	12.427	0.027	12.473	0.026	12.459	0.026	. . .
9..................	22533111−2005016	41.204	−62.157	11.09	10.87	10.746	0.022	10.748	0.024	10.752	0.021	+0.2
10..................	22574779−1822567	45.413	−62.456	11.83	11.91	12.209	0.026	12.323	0.028	12.317	0.030	. . .
11..................	22575321−3250528	12.887	−64.838	12.21	12.53	12.340	0.029	12.344	0.024	12.358	0.029	. . .
12..................	23010311−1805337	46.680	−63.043	11.41	11.38	11.377	0.022	11.391	0.025	11.424	0.026	. . .
13..................	23071216−3157380	14.589	−66.880	12.00	12.00	12.434	0.024	12.477	0.023	12.448	0.023	. . .
14..................	23091568−4123105	352.084	−64.679	11.39	11.28	11.169	0.021	11.211	0.024	11.186	0.021	+0.1
15..................	23223143−4559463	340.077	−64.200	12.05	12.29	12.531	0.022	12.558	0.026	12.582	0.023	−0.04
16..................	23270592−4009350	350.787	−68.234	13.90	13.30	13.177	0.023	13.203	0.026	13.244	0.033	. . .
17..................	23285991−1437024	61.878	−67.093	12.40	12.60	12.653	0.024	12.665	0.028	12.691	0.034	. . .
18..................	23334736−3853280	352.038	−69.988	11.57	11.51	11.489	0.023	11.531	0.023	11.544	0.024	. . .
19..................	23462825−3455590	359.615	−74.074	13.50	14.90	14.123	0.026	14.139	0.040	14.175	0.077	+0.03
20..................	23521950−3603516	353.839	−74.593	14.20	14.50	13.891	0.030	13.923	0.041	13.926	0.062	+0.03
21..................	23591014−4342306	332.011	−70.350	12.18	12.29	12.209	0.024	12.226	0.025	12.213	0.024	. . .
22..................	00152941−2105497	67.347	−79.825	12.15	12.40	12.242	0.023	12.316	0.025	12.326	0.023	. . .
23..................	00284278−1823502	90.819	−79.822	12.13	12.31	12.313	0.027	12.330	0.024	12.367	0.029	. . .
24..................	00284842−3632024	328.549	−79.443	13.50	13.90	13.686	0.032	13.717	0.029	13.772	0.060	. . .
25..................	00335405−4547026	312.367	−71.022	13.70	14.50	14.143	0.034	14.146	0.051	14.252	0.073	+0.1
26..................	00383181−3913183	314.660	−77.611	12.70	13.00	12.839	0.026	12.844	0.030	12.855	0.037	. . .
27..................	00471767−1453172	118.219	−77.722	13.20	14.00	14.110	0.032	14.132	0.033	14.199	0.064	. . .
28..................	00480632−4439565	304.897	−72.450	12.49	12.80	12.658	0.024	12.715	0.028	12.701	0.030	. . .
29..................	01011757−3342454	285.662	−83.082	. . .	. . .	13.232	0.026	13.361	0.028	13.431	0.043	−0.18
30..................	01090411−3307403	271.583	−82.894	11.91	12.03	12.444	0.022	12.570	0.028	12.621	0.037	. . .
31..................	01111697−2138541	163.494	−82.899	12.10	13.30	12.920	0.023	12.961	0.025	12.996	0.029	. . .
32..................	01142378−4710404	291.766	−69.450	12.48	12.59	12.365	0.024	12.382	0.023	12.379	0.026	. . .
33..................	01294009−4015539	274.303	−74.667	11.71	11.73	11.441	0.026	11.459	0.023	11.443	0.023	. . .
34..................	01511189−1732518	181.245	−73.210	11.68	11.46	11.578	0.023	11.610	0.023	11.617	0.026	. . .
35..................	02165824−3447583	240.943	−70.177	12.70	13.20	13.049	0.026	13.106	0.029	13.091	0.034	. . .
36..................	02192738−3637583	245.464	−69.107	12.40	13.00	12.665	0.023	12.696	0.029	12.701	0.029	. . .
37..................	02205977−3423353	239.155	−69.490	13.00	13.50	13.990	0.030	14.097	0.032	14.209	0.072	. . .
38..................	02221984−2324558	207.729	−69.149	11.78	11.99	12.616	0.026	12.748	0.021	12.842	0.031	. . .
39..................	02251836−2433280	211.264	−68.755	12.60	15.20	12.708	0.023	12.721	0.022	12.788	0.025	. . .
40..................	02272918−3953377	251.756	−66.375	11.83	12.07	12.197	0.024	12.212	0.026	12.288	0.024	. . .
41..................	02324780−2038431	202.761	−65.990	13.30	13.40	13.455	0.026	13.509	0.034	13.521	0.043	. . .
42..................	02344423−2108454	204.290	−65.735	12.00	12.10	12.291	0.026	12.299	0.025	12.297	0.026	+0.01
43..................	02484806−1500525	194.978	−60.165	11.04	11.21	11.251	0.026	11.319	0.022	11.309	0.021	. . .
44..................	02560556−3555579	239.150	−62.156	12.90	12.30	12.647	0.025	12.669	0.026	12.661	0.028	. . .

Notes.—The data are listed as they appear in the 2MASS point-source catalog. Col. (1): Order number. Col. (2): 2MASS name. Cols. (3) and (4): Galactic coordinates, in degrees. Cols. (5) and (6): Blue and red magnitudes. Cols. (7)–(12): J, σ_J, H, σ_H, K, and σ_K magnitudes. Col. (13): $B-V$ color, as given in the SIMBAD database.

mistaken for A0 stars. In terms of temperature, the values above imply that, for 1 σ error in the photometry, the minimum temperature in the sample must be 7900 K.

Although both color index restrictions include the J band, the use of two color indices simultaneously gives more reliability to the selection method. Besides, the magnitude criteria stated above also establish an upper limit for distance. This can be estimated assuming that (1) $M_J = +0.80$ (for HB stars; Brown et al. 2004), (2) $M_J \simeq M_K$, (3) there is negligible reddening toward the south Galactic pole in the three infrared bands, and (4) $K \leq 14.3$. Assuming these values, the upper limiting distance of the HB stars turns out to be 5.0 kpc. It does not differ much from the lower limit of the Sloan survey, which is near 7 kpc, imposed by saturation. Therefore, the Sloan survey and 2MASS complete each other with respect to the magnitude coverage.

Besides using the criteria cited above, due to limitations in the observation time only sources with declination in the range $-56.8° < \delta < -13.8°$, which corresponds to files aal through abv in the 2MASS database, have been selected. This set amounts to 218 2MASS sources and consists of approximately 80%–90% of the total number of objects with $\delta < -60°$. Once this first sample was defined, each object was searched for in the SIMBAD database for information about its nature, such as spectral type, luminosity class, UBV photometry, and counterparts in other catalogs. As mentioned in § 1, other similar surveys have been carried out (Beers et al. 1988, 1992, 1996; Wilhelm et al. 1999a, 1999b; Brown et al. 2003; Sirko et al. 2004), and this study is mainly aimed at stars which have been overlooked in previous surveys. Higher priority is given to objects without any information in the SIMBAD database, especially concerning their spectral

TABLE 2
Log Book of the Observations

Night	Date	Julian Date	Telescope Size (m)
1........................	2003 Oct 25	2,452,938	1.60
2........................	2003 Oct 26	2,452,939	1.60
3........................	2003 Oct 27	2,452,940	1.60
4........................	2003 Nov 10	2,452,954	0.60
5........................	2003 Nov 11	2,452,955	0.60
6........................	2004 Sep 4	2,453,253	0.60
7........................	2004 Sep 5	2,453,254	0.60
8........................	2004 Sep 6	2,453,255	0.60

classification. Forty-four sources fulfilling the criteria above were selected for observation and are listed in Table 1, as they appear in the 2MASS point-source catalog. Since the beginning of the observation runs a few of these stars have been observed and classified by other authors; these cases are noted throughout this paper.

3. OBSERVATIONS

Observations were carried out at the Pico dos Dias Observatory, operated by the National Laboratory for Astrophysics (LNA) located in Itajubá, southeast Brazil, during several runs between 2003 and 2005. Two different Boller & Chivens telescopes were used: a 1.60 m and a 60 cm, both equipped with the same Cassegrain spectrograph. A long east-west slit of 2″ width was used in all observations. The effective focus ratio was f/13.5 on both telescopes, resulting in a reciprocal dispersion of 1.2 Å pixel^{-1} with the 600 line mm^{-1} grid used.

Table 2 lists the log book of the observations. Image reduction and analysis were performed using the IRAF package,[2] including the classical procedure to reduce long-slit spectra: bias, dark, and flat-field corrections; spectral profile extraction; and wavelength calibration, which was derived using a He-Ar lamp. After continuum normalization, equivalent widths were calculated assuming Voigt profiles, and a deblending routine was used when necessary. The Voigt profiles were fitted for each diagnostic line using the IRAF `splot` algorithm. The profile is centered on the line minimum and constrained by the local pseudocontinuum, which is defined by the average values taken from 10 Å wide windows located 25 Å on either side of the line minimum.

4. RESULTS

Figure 2 shows the normalized spectra of the 44 stars observed, ordered by right ascension, as displayed in Table 1. Table 3 lists the characteristics of the Balmer series, as well as the Ca II K line, according to the definitions proposed by Pier (1983) and Beers et al. (1992) to classify stars among subdwarfs, the HB, degenerate stars, and the MS. The equivalent widths (W), $D_{0.2}$, R, and HP index have all been obtained by fitting a Voigt profile to the lines and are listed in Table 3. Among them, two parameters are more suited to classify the star: the Hδ R-index, which is the

---

[2] IRAF is distributed by the National Optical Astronomy Observatory, which is operated by the Association of Universities for Research in Astronomy, Inc., under contract to the National Science Foundation.
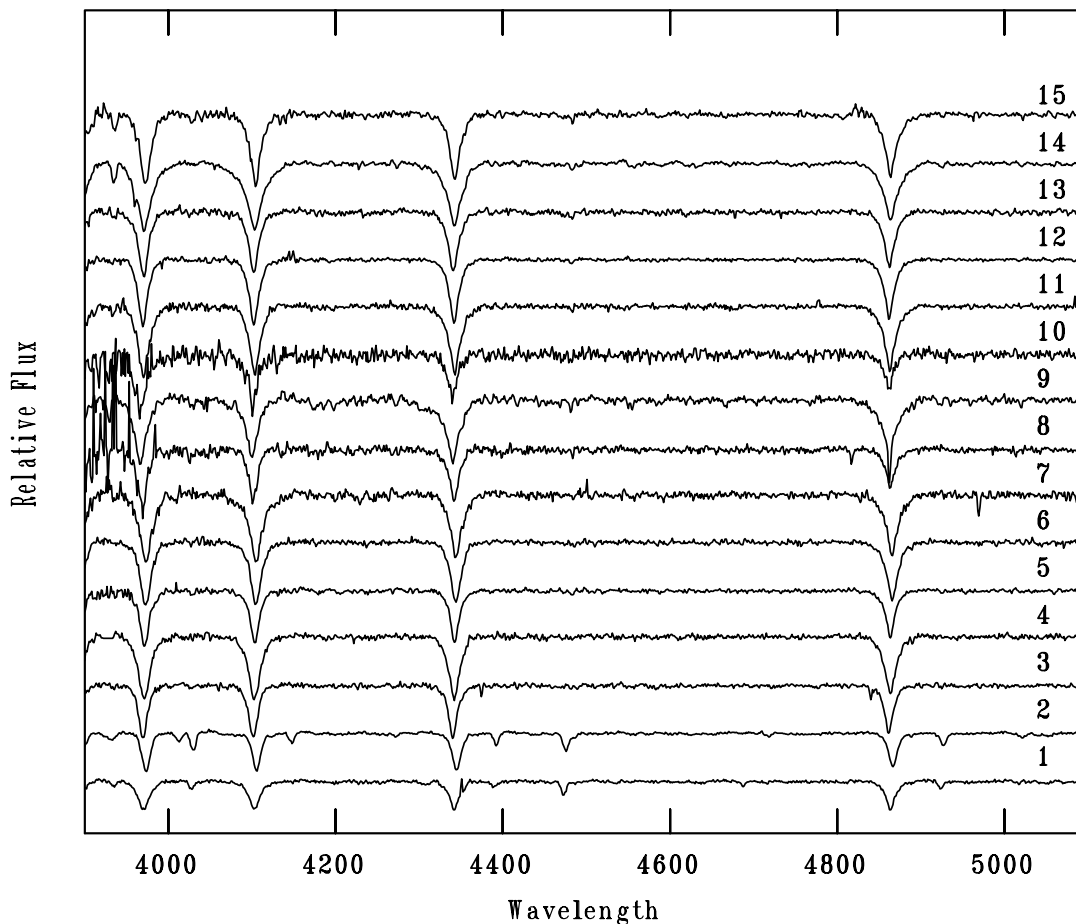

Fig. 2.—Observed spectra of the sample, with their continua normalized. Each number (*right-hand side*) corresponds to the order given in Table 1.
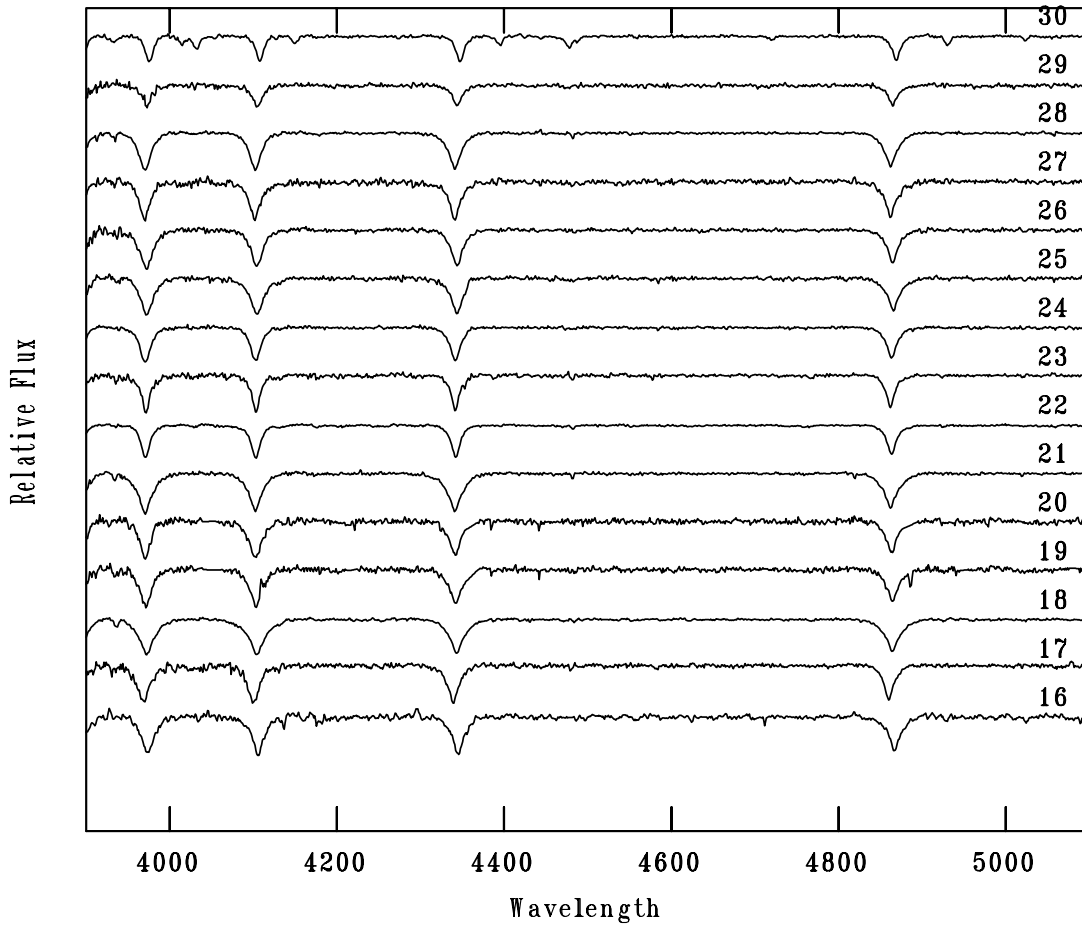
Fig. 2—*Continued*

ratio between the continuum and the "depth" of the line, and $D_{0.2}$, which is the width of the line taken at 0.8 times the intensity of the continuum (Pier 1983; Wilhelm et al. 1999a). The preference for Hδ over Hγ to perform the calculation of R and $D_{0.2}$ is justified because of the G band near ∼4300 Å, which might affect the determination of the continuum near the Hγ line, especially among the cooler stars of the sample (Wilhelm et al. 1999a). Stars of each type appear distributed in characteristic regions in the R versus $D_{0.2}$ diagram (Fig. 3), although some of the types may appear mixed up, sharing the same portion of the diagram. According to this diagram, five stars belong to the subdwarf category: 22361663−3142130, 22385421−2352209, 01011757−3342454, 02205977−3423353, and 02221984−2324558, whereas all the remaining objects are either A stars or FHB objects. Table 4, which lists the stars with He lines detected, together with the photometric data of Table 1, gives additional information that helps to clarify the nature of these objects. They are discussed in more detail later in this paper. As for the remaining stars, Figure 3 does not allow a reliable classification. The right side of the diagram gathers both the candidate FHB and A stars. As the numerous references in the literature claim (Pier 1983; Sommer-Larsen & Christensen 1986; Wilhelm et al. 1999a), separating these two classes of objects is difficult because both share the same locus in the R versus $D_{0.2}$ diagram. Nevertheless, there are four objects with $D_{0.2} > 35$ Å, which are far more likely to be A stars.

To disentangle FHB and A stars, the derivation of both the stellar temperature and log g becomes necessary. The $B - V$ color index is a widely known temperature estimator; however, as Table 1 shows, this information is available for only a few sources. On the other hand, near-infrared photometry is available for all sources, but in spite of several attempts to derive the temperature of hot stars using the *JHK* color indices (Koornneef 1983; Beers et al. 2007), this method is inaccurate, because the spectral energy distribution approaches the Rayleigh-Jeans regime in the near-infrared. In this study the temperature and gravity of each star have been determined simultaneously, comparing characteristics of the Hβ, Hγ, and Hδ features with a grid of synthetic spectra calculated by R. L. Kurucz (1993, private communication) assuming solar metallicity and the following ranges of temperature and gravity: 7000 K $\leq T_{\rm eff} \leq$ 12,000 K and 2.0 $\leq$ log $g \leq$ 5.0, with increments of $\Delta T = 250$ K for $T_{\rm eff} \leq$ 10,000 K, $\Delta T = 500$ K for $T_{\rm eff} > 10,000$ K, and Δlog $g = 0.5$ in all cases. The spectral parameters that were compared with the models are the equivalent widths (W) of Hβ, Hγ, and Hδ and the $D_{0.2}$ of Hγ and Hδ. This choice is justified because the Balmer lines are sensitive to both temperature and gravity, which are the main scope of this study. The total χ^2 is calculated according to the equation

$$\chi^2 = \frac{[W(\mathrm{H}\beta)_* - W(\mathrm{H}\beta)_K]^2}{\sigma^2(W(\mathrm{H}\beta))} + \frac{[W(\mathrm{H}\gamma)_* - W(\mathrm{H}\gamma)_K]^2}{\sigma^2(W(\mathrm{H}\gamma))}$$
$$+ \frac{[W(\mathrm{H}\delta)_* - W(\mathrm{H}\delta)_K]^2}{\sigma^2(W(\mathrm{H}\delta))} + \frac{[D_{0.2}(\mathrm{H}\gamma)_* - D_{0.2}(\mathrm{H}\gamma)_K]^2}{\sigma^2(D_{0.2}(\mathrm{H}\gamma))}$$
$$+ \frac{[D_{0.2}(\mathrm{H}\delta)_* - D_{0.2}(\mathrm{H}\delta)_K]^2}{\sigma^2(D_{0.2}(\mathrm{H}\delta))}, \tag{1}$$

where σ is the error bar of the measurement, typically 1/10 of W and $D_{0.2}$. The asterisk and "K" subscripts correspond to observation
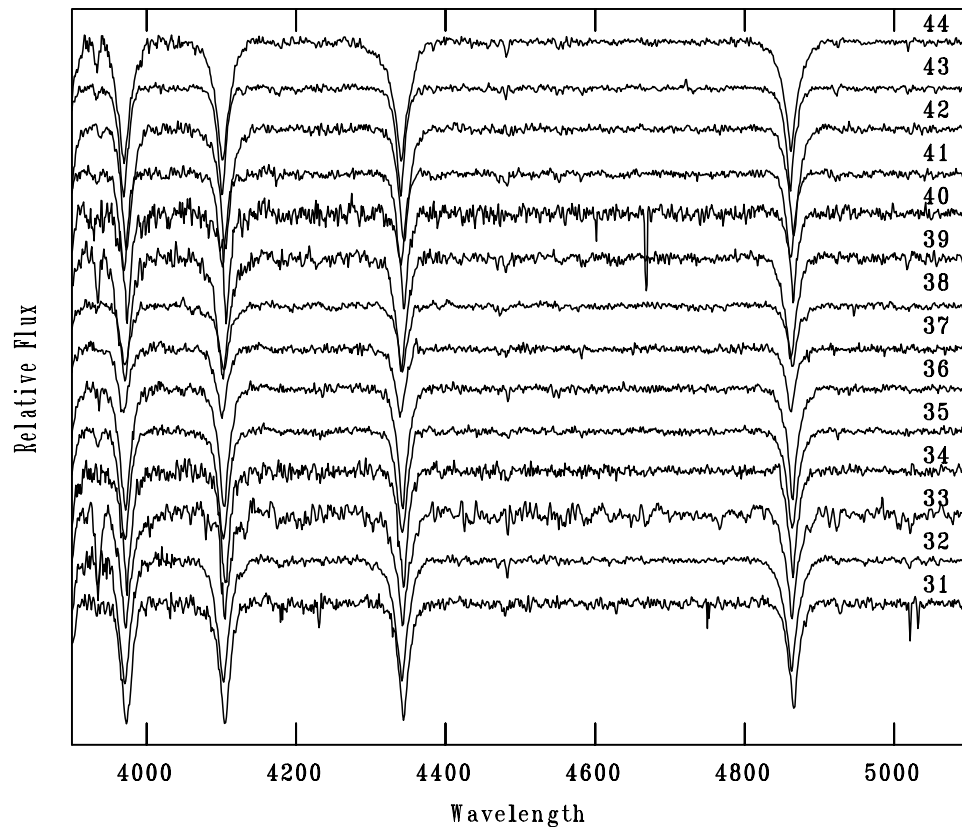
FIG. 2—*Continued*

and model, respectively. It is well known that the hydrogen lines present a maximum in intensity near the A2 spectral type. As a consequence, for a given value of log g, there are frequently two solutions for T_{eff}, corresponding to the two local minima of χ^2. Considering also the range of log g, the number of local minima can be even higher.

We carried out the calculation of χ^2 for the whole range of temperature and gravity defined above. In a certain number of cases, when He lines were present or $B - V$ was available, we were able to identify the correct solution among the various local minima. In other cases, when the Ca II K line was detected, W_K was used to discard local χ^2 minima whose temperatures were incompatible with the theoretical models. This was done using the T_{eff} versus W_K diagram proposed by Wilhelm et al. (1999a), calculated for a wide range of temperature and metallicities, which is based on Kurucz's grid of models previously cited in this section. For stars with W_K measurements, incorrect (T_{eff}, log g) solutions were discarded if their measured W_K was incompatible with the synthetic figure corresponding to that temperature (Fig. 2 of Wilhelm et al. 1999a). Nevertheless, even all these techniques together left a considerable number of stars with multiple solutions of T_{eff} and log g. All single and multiple solutions are presented in Table 5, which includes all sources observed, except those previously identified as subdwarfs according to the diagram depicted in Figure 3.

In order to test the method used for determining the stellar temperatures, we applied it to a test sample, containing stars with temperatures previously determined by a distinct technique. Wilhelm et al. (1999b) determined the T_{eff} of a sample of FHB stars using a hybrid method that makes use of the $B - V$ and $U - B$ colors, as well as $D_{0.2}$ of Hδ and Hγ (Wilhelm et al. 1999a). According to that method, synthetic values are obtained from the models proposed by R. L. Kurucz (1993, private communication), which

are compared with the values obtained from the observations, according to a pondering function that varies with the temperature. Figures 4a and 4b show the stellar temperatures of a subsample of FHB stars (collected from the list published by Wilhelm et al. 1999b) calculated by both methods. A clear bias seems to exist, showing that the present method produces higher temperatures when compared with the results of Wilhelm et al. (1999b). A similar bias was noticed by Kinman & Castelli (2002), who used V, J, H, and K magnitudes to calibrate a gravity- *and* metallicity-dependent relationship between these color indices and T_{eff}. According to that study, the temperatures determined by Wilhelm et al. (1999b) are systematically cooler than those determined from the 2MASS color indices by an amount that increases with T_{eff}.

Since $B - V$ and $E(B - V)$ are both available for practically all the stars in the sample of Wilhelm et al. (1999b), we also compared our method with a well-established relationship between $(B - V)_0$ and T_{eff}. This relationship (Gray 1992) was found from observations carried out by various authors who obtained UBV photometry relative to stars in a wide range of gravities and temperatures. We did not use the relationships proposed by Kinman & Castelli (2002), because a comparison between B and V magnitudes taken from the 2MASS catalog and the same magnitudes measured by other authors (available in the literature) shows large error bars for magnitudes beyond $B = 11.0$.

Figures 4c and 4d show that no large bias seems to exist between the temperatures determined in this work and those obtained using the $(B - V)_0$ versus T_{eff} relationship, within the temperature range 7000 K $< T_{\mathrm{eff}} <$ 12,000 K. The difference $\Delta T = T_{\mathrm{this\ work}} - T_{B-V}$ follows a Gaussian distribution centered at $\Delta T = -180$ K and half-width $\sigma = 700$ K. However, this scattering does not result only from the uncertainty of the present method, but is also due to some scattering present in the $(B - V)_0$ versus T_{eff} relationship. Although Gray (1992) points out that no

TABLE 3
CHARACTERISTICS OF THE HYDROGEN FEATURES IN THE SPECTRA

2MASS NAME	W (VOIGT) (Å)			$D_{0.2}$		R		HP INDEX	W (VOIGT) Ca II K (Å)	NIGHT
(1)	Hβ (2)	Hγ (3)	Hδ (4)	Hγ (5)	Hδ (6)	Hγ (7)	Hδ (8)	(9)	(10)	(11)
22361663−3142130	6.1	5.3	6.8	8.7	10.5	0.29	0.28	6.2	...	1
22385421−2352209	6.0	6.2	5.6	11.7	11.1	0.38	0.39	6.2	...	2
22393762−2455025	9.6	10.0	10.2	15.9	18.1	0.55	0.56	10.7	...	4
22475352−3829408	15.1	14.2	16.0	23.3	23.5	0.67	0.66	16.1	...	1
22480188−3503104	9.5	10.0	13.4	15.4	19.4	0.54	0.57	12.3	...	5
22501122−3759588	14.5	12.2	14.8	21.2	22.3	0.62	0.65	14.3	...	2
22515349−4355577	15.9	18.0	21.6	27.7	29.1	0.67	0.71	21.1	...	5
22524524−2147476	8.6	12.2	12.3	20.2	20.1	0.55	0.60	13.0	...	6
22533111−2005016	19.7	17.2	23.3	26.7	33.0	0.61	0.60	21.5	1.30	6
22574779−1822567	8.1	11.7	8.2	18.0	11.6	0.55	0.64	10.7	...	6
22575321−3250528	15.9	17.9	19.7	26.4	29.6	0.73	0.75	20.1	0.50	6
23010311−1805337	12.7	13.6	14.8	20.3	23.3	0.67	0.69	15.1	...	6
23071216−3157380	12.0	14.9	17.1	23.0	25.7	0.62	0.66	17.0	...	4
23091568−4123105	20.9	19.3	24.0	30.0	36.3	0.66	0.70	23.1	1.30	3
23223143−4559463	14.2	13.4	16.0	20.7	23.3	0.68	0.76	15.6	0.89	7
23270592−4009350	17.4	19.8	24.8	31.4	34.8	0.71	0.75	23.8	...	4
23285991−1437024	14.0	16.3	10.1	23.6	19.2	0.70	0.66	14.4	...	7
23334736−3853280	19.9	20.5	25.4	32.2	38.0	0.64	0.67	24.5	0.96	5
23462825−3455590	15.7	17.6	15.2	26.7	19.8	0.62	0.70	17.7	...	3
23521950−3603516	14.6	15.2	16.9	23.2	25.6	0.62	0.66	17.1	...	3
23591014−4342306	20.0	21.3	25.5	32.7	38.0	0.72	0.74	25.0	0.51	8
00152941−2105497	10.9	10.7	11.0	17.6	17.2	0.59	0.60	11.5	...	3
00284278−1823502	11.3	10.9	9.7	15.6	16.6	0.65	0.67	11.0	0.46	7
00284842−3632024	12.7	12.8	13.6	20.6	21.5	0.61	0.62	14.1	...	2
00335405−4547026	16.1	14.6	19.4	24.3	27.5	0.66	0.65	18.0	...	2
00383181−3913183	16.1	17.1	22.2	26.5	29.7	0.68	0.70	20.9	...	4
00471767−1453172	15.4	16.1	17.0	24.4	22.9	0.72	0.73	17.7	...	8
00480632−4439565	17.0	18.2	20.5	26.3	29.8	0.69	0.72	20.7	0.24	8
01011757−3342454	8.3	9.5	13.3	14.0	18.6	0.39	0.45	12.0	...	4
01090411−3307403	7.8	7.6	8.6	16.0	13.2	0.44	0.67	8.5	...	5
01111697−2138541	14.9	15.8	17.7	30.5	23.3	0.68	0.72	17.9	...	5
01142378−4710404	20.3	21.7	23.4	32.7	33.7	0.71	0.73	24.2	0.72	8
01294009−4015539	17.0	17.4	...	29.7	...	0.65	...	59.9	4.50	7
01511189−1732518	12.3	13.0	9.1	19.6	16.5	0.68	0.63	11.9	...	7
02165824−3447583	14.7	12.3	16.9	21.9	24.9	0.59	0.63	15.4	0.53	2
02192738−3637583	16.1	17.6	21.2	27.8	30.4	0.71	0.71	20.7	0.31	8
02205977−3423353	8.9	8.1	10.8	15.1	17.8	0.39	0.41	9.9	...	2
02221984−2324558	8.4	8.1	9.8	13.5	16.2	0.39	0.38	9.4	...	3
02251836−2433280	15.7	18.7	22.3	28.7	31.9	0.68	0.72	21.9	1.23	4
02272918−3953377	9.1	10.1	6.1	16.4	10.1	0.56	0.59	8.7	...	7
02324780−2038431	10.2	9.4	10.1	15.9	16.8	0.53	0.55	10.3	...	2
02344423−2108454	15.2	18.1	21.5	26.3	30.4	0.67	0.71	21.1	...	4
02484806−1500525	12.8	12.7	13.9	19.6	21.1	0.64	0.64	14.1	0.39	8
02560556−3555579	21.2	23.9	27.0	36.6	39.6	0.70	0.72	27.3	1.08	8

NOTES.—Col. (1): Name of the 2MASS source. Cols. (2)–(4): Voigt equivalent widths of the Hβ, Hγ, and Hδ lines, respectively. Cols. (5) and (6): $D_{0.2}$ of the Hγ and Hδ lines, respectively. Cols. (7) and (8): R of Hγ and Hδ, respectively. Col. (9): HP index, defined by Pier (1983), Sommer-Larsen & Christensen (1986), and Wilhelm et al. (1999a). Col. (10): Voigt equivalent width of the Ca II K line. Col. (11): Night number (see Table 2).

clear dependence seems to exist on log g or [Fe/H], an intrinsic scattering resulting from the various observational conditions is present. This scattering varies with $(B − V)_0$, being typically 2%–3% of the temperature for an increment $\sigma(B − V)_0 = 0.01$, but it might be as high as 4% if $(B − V)_0 < 0.0$. In fact, a good determination of the dereddened $(B − V)_0$ requires, besides good photometric observations, an accurate estimation of the color excess $E(B − V)$. These two effects combined, and assuming $\sigma(B − V)_0 = 0.01$, imply an uncertainty in temperature of 200 K at $T_{\mathrm{eff}} = 7000$ K or 440 K for $T_{\mathrm{eff}} = 12,000$ K. Part of the width of the ΔT distribution observed in Figure 4d (half-width $\sigma = 700$ K) is due to this effect, whereas another part is caused by the error of

the present method only. Thus, we conclude that the intrinsic error bar of the method for determining T_{eff} proposed in this work, which is not based on $(B − V)_0$ but on some features of the Balmer series, is about 500 K, on average.

Figure 5 illustrates a well-known tool proposed by Wilhelm et al. (1999a) to visualize the stellar parameters T_{eff} and log g. The input data to this plot are given in Table 5. The uniquely determined solutions of T_{eff} and log g are shown as filled circles, whereas the multiple solutions are shown as open circles. An examination of Figure 5 reveals that the stars in the sample are distributed over a wide range of gravities, $2.0 \leq \log g \leq 5.0$. This excludes low-gravity objects such as post-AGB stars, which are
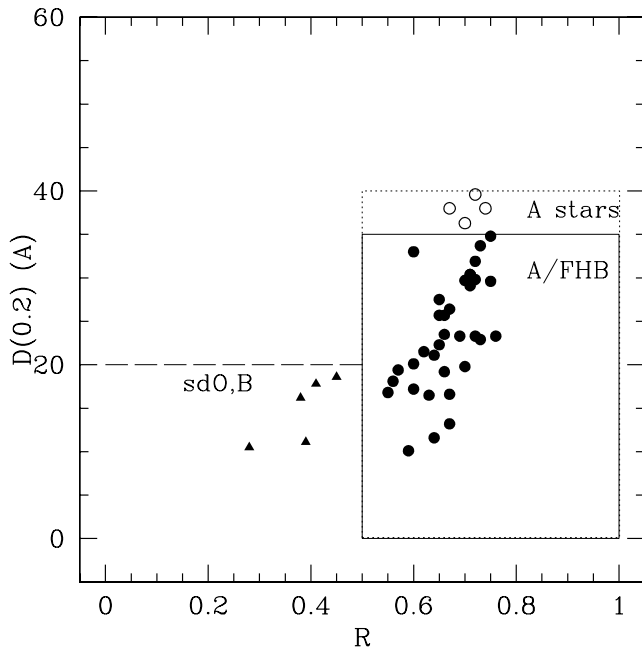
FIG. 3.—Sample in R vs. Hδ $D_{0.2}$, calculated using the Hδ line as given in Table 3. The symbols used in this preliminary classification are as follows: sdO, sdB (*triangles*), A/FHB stars (*filled circles*), and MS A stars (*open circles*).

often discovered at high latitudes, as in this survey. The range of $\log g$ values also excludes degenerate stars such as white dwarfs. On the other hand, the range of $\log g$ does include both FHB and A stars and, in a limited number of cases, allows discrimination between these two categories. This especially applies to the objects located on the right side of the diagram, where $T_{\rm eff} < 10,000$ K, and the four objects in the upper box of Figure 3.

Unfortunately, because the sample was mainly aimed at objects overlooked in previous surveys, no data on radial velocity exist in the literature, except in the cases of 23462825−3455590 and 23521950−3603516 (Wilhelm et al. 1999b).

4.1. Subdwarfs

As noted above, five stars are classified as subdwarfs according to the R versus $D_{0.2}$ diagram. The star 22361663−3142130 was previously identified as a subdwarf (Kilkenny et al. 1988). The several He I and He II lines present in its spectrum (Table 4) and its $B - V$ color index (Table 1) support its classification as an sdO star. The star 22385421−2352209 has numerous He I lines, but He II is absent. Its $B - V$ color is also consistent with its classification as an sdB star. The star 01011757−3342454 does not show He lines in the present spectrum, perhaps because of its

low S/N. Nevertheless, this object is a well-known sdB star showing high radial velocity (Bergeron et al. 1984; Altmann et al. 2004; Edelmann et al. 2005). Its position in the R versus $D_{0.2}$ diagram only confirms its previous classification. The spectrum of 02221984−2324558 exhibits the He I λ4471 line, suggesting its classification as sdB. It has been recently cataloged as a subdwarf B binary in the Edinburgh-Cape survey (Morales-Rueda et al. 2006). Like 02221984−2324558, the star 02205977−3423353 was only recently classified as sdB (Altmann et al. 2004), after the beginning of the present survey. Table 1 tells us that it is one of the faintest objects in the sample. Its He I lines remain undetected, probably because of the low S/N and the fact that the Balmer lines in subdwarfs are typically shallow.

4.2. A-Type Stars

Figure 3 shows four stars that appear in the region of the R versus $D_{0.2}$ diagram where only A-type stars are commonly found. None of them have been previously confirmed as A stars. These objects are 23091568−4123105, 23334736−3853280, 23591014−4342206, and 02560556−3555579. Table 5 shows $\log g \geq 4.0$ for all of them, confirming this classification. The measurement of the Ca II K line helped to remove the degeneracy of the multiple solutions of $T_{\rm eff}$ of the following stars: 23091568−4123105, 23591014−4342206, and 23334736−3853280. According to the theoretical models, the strength of the Ca II K line indicates that the former two objects have subsolar [Fe/H], whereas the latter probably has nearly solar metallicity.

Besides the A stars clearly classified using the R versus $D_{0.2}$ diagram, there are several borderline cases showing Hδ $D_{0.2}$ in the range 30–35 Å. The stars belonging to this category are 22533111−2005016, 23270592−4009350, 01142378−4710404, 02192738−3637583, 02251836−2433280, and 02344423−2108454. The objects 22533111−2005016 and 02251836−2433280 both exhibit strong Ca II K lines, which discards the χ^2 high-temperature solution, confirming them as A-type stars. The theoretical models indicate that 01142378−4710404 and 02192738−3637583 must be low-metallicity stars. Considering what has been exposed above, one can state that the former three objects are confirmed A stars, whereas the latter three are in fact borderline cases, because their χ^2 solutions are compatible with both A and FHB classifications. Among them, only 02344423−2108454 has been previously observed in some detail (Kilkenny & Muller 1989; Kilkenny 1995). There are no Hδ measurements for the star 01294009−4015539 which could allow its classification using the method applied to the other stars in the sample. However, its Hγ line characteristics suggest that it might be either an A or a FHB star. On the other hand, the high intensity of the Ca II K line suggests that its metallicity is near solar,

TABLE 4
EQUIVALENT WIDTHS (Å) OF THE HELIUM LINES DETECTED IN THE SURVEY

2MASS Name	He I λ4009	He I λ4026	He I λ4144	He I λ4388	He I λ4471	He I λ4922	He II λ4686
22361663−3142130	. . .	0.61	. . .	0.41	0.98	0.59	0.34
22385421−2352209	0.86	1.51	0.81	0.99	2.01	1.18	. . .
22524524−2147476	. . .	0.32	. . .	. . .	. . .	. . .	. . .
01090411−3307403	1.81	2.15	1.11	1.65	2.98	1.36	. . .
01111697−2138541	. . .	. . .	. . .	. . .	. . .	0.51	. . .
02165824−3447583	. . .	. . .	. . .	. . .	. . .	0.12	. . .
02221984−2324558	. . .	. . .	. . .	. . .	0.16	. . .	. . .
02324780−2038431	. . .	. . .	. . .	. . .	0.18	. . .	. . .

NOTE.—All lines have been fitted using a Voigt profile.

TABLE 5

STELLAR TEMPERATURE AND GRAVITY OF THE OBJECTS SURVEYED

2MASS Name	Hδ $D_{0.2}$ (Å)	T_1 (K)	log g	χ_1^2	T_2 (K)	log g	χ_2^2	T_3 (K)	log g	χ_3^2	Class
22393762−2455025	18.1	>17000	4.5	2.7	. . .	. . .	. . .	. . .	. . .	. . .	A
22475352−3829408	23.5	7750	3.0	1.8	12500	4.5	0.7	. . .	. . .	. . .	. . .
22480188−3503104	19.4	7500	4.5	15.7	10000	3.0	15.4	11500	3.5	11.4	. . .
22501122−3759588...........	22.3	7500	3.0	5.2	10000	3.5	5.2	11500	4.0	3.5	. . .
22515349−4355577	29.1	8250	3.5	3.8	11000	4.5	4.0	. . .	. . .	. . .	. . .
22524524−2147476	20.1	11500	3.5	21.1	13000	4.0	15.5	16000	4.5	14.3	. . .
22533111−2005016...........	33.0	8250	4.0	6.9	. . .	. . .	. . .	. . .	. . .	. . .	A
22574779−1822567	11.6	7000	3.5	18.6	11000	3.0	18.1	13000	3.5	15.1	. . .
22575321−3250528[a]	29.6	8250	3.5	2.8	. . .	. . .	. . .	. . .	. . .	. . .	FHB
23010311−1805337...........	23.3	7500	4.0	6.6	10000	3.5	5.0	13000	4.5	2.0	. . .
23071216−3157380	25.7	7750	3.0	12.1	8750	3.0	14.2	10000	3.5	12.8	. . .
23091568−4123105	36.3	8500	4.0	3.1	. . .	. . .	. . .	. . .	. . .	. . .	A
23223143−4559463	23.3	10000	3.5	3.7	. . .	. . .	. . .	. . .	. . .	. . .	. . .
23270592−4009350	34.8	8500	4.0	4.0	. . .	. . .	. . .	. . .	. . .	. . .	A
23285991−1437024...........	19.2	7500	4.0	13.6	9250	3.0	16.0	. . .	. . .	. . .	. . .
23334736−3853280	38.0	9500	4.5	3.6	. . .	. . .	. . .	. . .	. . .	. . .	A
23462825−3455590	19.8	8750	3.0	3.9	. . .	. . .	. . .	. . .	. . .	. . .	FHB
23521950−3603516	25.6	7750	3.0	2.5	12000	4.5	1.4	. . .	. . .	. . .	. . .
23591014−4342306	38.0	9500	4.5	2.5	. . .	. . .	. . .	. . .	. . .	. . .	A
00152941−2105497	17.2	7500	4.5	2.2	11500	3.5	2.7	13000	4.0	1.6	. . .
00284278−1823502	16.6	7000	3.0	3.0	7500	4.5	2.8	10000	3.0	2.8	. . .
00284842−3632024	21.5	7500	4.0	4.4	14000	4.5	1.1	. . .	. . .	. . .	. . .
00335405−4547026	27.5	8250	3.0	5.8	12000	4.5	4.5	. . .	. . .	. . .	. . .
00383181−3913183	29.7	8250	3.5	5.2	10000	4.0	5.4	. . .	. . .	. . .	. . .
00471767−1453172	22.9	7750	3.0	0.7	8500	3.0	0.7	12000	4.5	0.6	. . .
00480632−4439565[a]	29.8	8250	3.5	1.8	11000	4.5	2.0	. . .	. . .	. . .	. . .
01090411−3307403...........	13.2	11500	3.0	11.1	. . .	. . .	. . .	. . .	. . .	. . .	FHB
01111697−2138541...........	23.3	10500	4.0	5.8	12000	4.5	5.5	. . .	. . .	. . .	. . .
01142378−4710404...........	33.7	8750	4.5	0.7	10000	4.5	0.5	. . .	. . .	. . .	A
01511189−1732518...........	16.5	7500	4.5	7.8	. . .	. . .	. . .	. . .	. . .	. . .	A
02165824−3447583	24.9	10000	3.5	9.7	. . .	. . .	. . .	. . .	. . .	. . .	. . .
02192738−3637583	30.4	8250	3.5	3.8	11000	4.5	3.8	. . .	. . .	. . .	A
02251836−2433280	31.9	8500	3.5	6.4	. . .	. . .	. . .	. . .	. . .	. . .	A?
02272918−3953377	10.1	7000	4.5	16.4	. . .	. . .	. . .	. . .	. . .	. . .	A
02324780−2038431	16.8	12000	3.5	3.8	14000	4.0	2.8	17000	4.5	1.3	. . .
02344423−2108454	30.4	10000	4.0	6.5	. . .	. . .	. . .	. . .	. . .	. . .	A
02484806−1500525	21.1	7500	4.0	4.3	9250	3.0	4.2	10500	3.5	3.1	. . .
02560556−3555579	39.6	9250	4.5	2.1	. . .	. . .	. . .	. . .	. . .	. . .	A

NOTES.—Subdwarfs excluded. Temperatures T_1, T_2, and T_3 correspond to the various least-χ^2 values calculated using eq. (1). The error bars of T and log g are 500 K and 0.5 dex, respectively.

[a] Considering the strength of the Ca II K line and the assumption of $T_{\rm eff}$ = 8250 K and log g = 3.5, this must be a low-metallicity star.
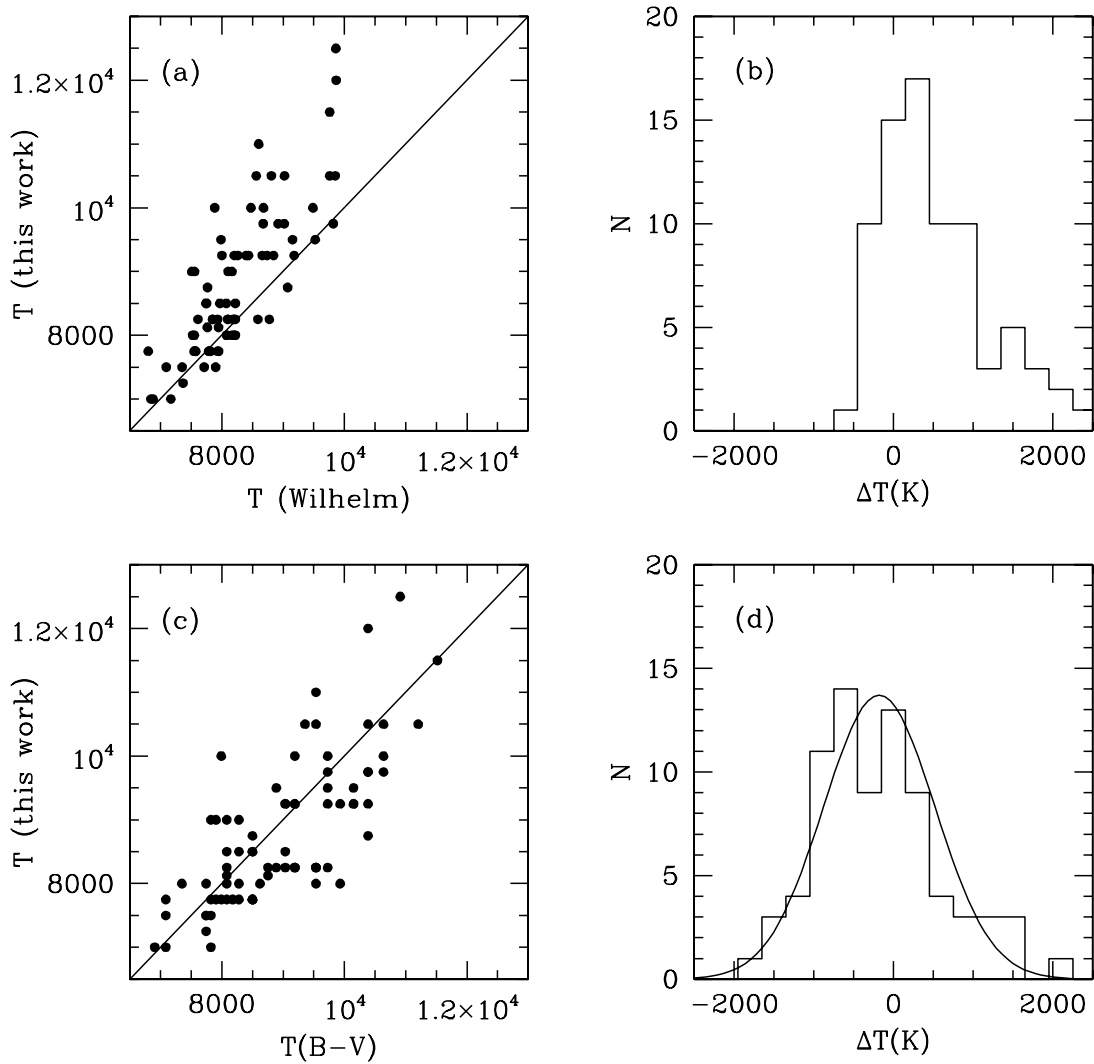
FIG. 4.—(*a, b*) Comparison between the stellar T_{eff} determined in this work and by Wilhelm et al. (1999b). (*c, d*) Same as (*a*) and (*b*), but using the $(B - V)_0$ vs. T_{eff} relationship by Gray (1992). In both cases ΔT represents the difference between the temperature calculated in the present work (based on Kurucz's models) and the other method.
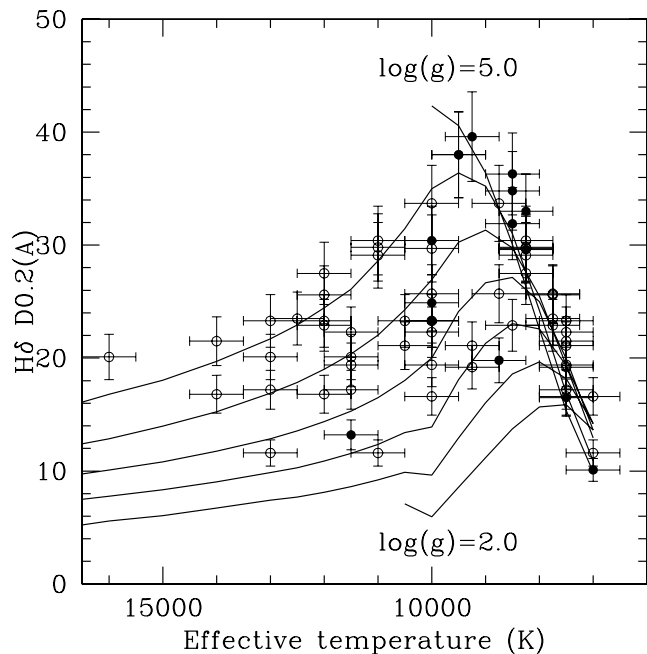
Fig. 5.—Plot of $T_{\rm eff}$ vs. Hδ $D_{0.2}$ (Å). Surface gravity and temperature correspond to the least-χ^2 values calculated using eq. (1) and given in Table 5. Filled circles represent the unique solutions of $T_{\rm eff}$ and log g, whereas open circles represent all the remaining multiple solutions. The lines represent the model atmospheres by Kurucz for various log g values and solar metallicity. Stars identified as subdwarfs in Fig. 3 have been omitted.

which favors the A-type classification. Other stars in Table 5 likely to be A types have been classified according to their log g values.

The *JHK* magnitudes can be used to calculate the distance to the Galactic plane of these stars. Assuming the infrared color indices for the MS given by Koornneef (1983), all objects reliably classified as A type are in the range 0.7 kpc $< |z| <$ 2.3 kpc and therefore immersed in the thick disk traced by Gilmore & Reid (1983). According to that study, the thick-disk population dominates over the thin disk beyond $|z| > 1.5$ kpc, which corresponds to the average $|z|$ value of the A-type stars of the present sample.

4.3. *FHB Stars*

FHB stars frequently appear mixed with A-type stars, especially beyond $T_{\rm eff} = 10{,}000$ K. Disentangling these two kinds of objects is a cumbersome task, as discussed in § 1. We have identified only two objects in the sample that can accurately be clas-

sified as FHB stars based on their log g and $T_{\rm eff}$: 23462825−3455590 and 01090411−3307403. The former (CS 22941−0050) has been previously confirmed as a halo FHB object by Wilhelm et al. (1999b), who determined the following characteristics for this star: $D = 4.2$ kpc, $T_{\rm eff} = 8739$ K, log $g = 3.0$, and [Fe/H] = −1.7. Assuming $M_J = +0.80$ (Brown et al. 2004) and using the 2MASS *J* magnitude, we estimate its distance as 4.6 kpc, and the least-χ^2 solution indicates $T_{\rm eff} = 8750$ K and log $g = 3.0$ (Table 5), in full agreement with Wilhelm et al.'s results. The latter object has not been studied before, but its *J* magnitude and its classification as a FHB star imply $D = 2.1$ kpc, immersed in the Galactic halo. There also seems to be a third object, 22575321−3250528, that can been classified as FHB based on its low metallicity, deduced from log g, $T_{\rm eff}$, and the intensity of its Ca II K line.

The remaining objects omitted here and in the two previous sections cannot be reliably classified. Additional observations, especially *UBV* photometry, may help to figure out log g and $T_{\rm eff}$ among the multiple solutions; however, even these new data would leave a significant fraction of the sample unclassified.

5. CONCLUSIONS

We carried out a low-resolution spectroscopic survey of hot stars toward the southern Galactic pole, chosen according to their *JHK* 2MASS color indices. Forty-four stars were observed and had their temperature and surface gravity determined by fitting some of their Balmer features with a grid of model atmospheres. Five objects are classified as subdwarfs, 12 are classified as A stars, and 3 can be reliably classified as FHB objects. The nature of the remaining objects cannot be accurately determined, either because their log g and $T_{\rm eff}$ are compatible both with A and FHB types or because of the lack of *UBV* photometry, which would allow the correct determination of their temperature.

REFERENCES

Altmann, M., Edelmann, H., & de Boer, K. S. 2004, A&A, 414, 181
Beers, T. C., Almeida, R., Rossi, S., Wilhelm, R., & Marsteller, B. 2007, ApJS, 168, 277
Beers, T. C., Preston, G. W., & Shectman, S. A. 1988, ApJS, 67, 461
Beers, T. C., Preston, G. W., Shectman, S. A., Doinidis, S. P., & Griffin, K. E. 1992, AJ, 103, 267
Beers, T. C., Wilhelm, R., Doinidis, S. P., & Mattson, C. J. 1996, ApJS, 103, 433
Behr, B. B. 2003, ApJS, 149, 67
Bergeron, P., Fontaine, G., Lacombe, P., Wesemael, F., Crawford, D. L., & Jakobsen, A. M. 1984, AJ, 89, 374
Bessell, M. S., & Brett, M. 1988, PASP, 100, 1134
Brown, W. R., Allende Prieto, C., Beers, T. C., Wilhelm, R., Geller, M. J., Kenyon, S. J., & Kurtz, M. J. 2003, AJ, 126, 1362
Brown, W. R., Geller, M. J., Kenyon, S. J., Beers, T. C., Kurtz, M. J., & Roll, J. B. 2004, AJ, 127, 1555
Conlon, E. S., Dufton, P. L., Keenan, F. P., & Leonard, P. J. T. 1990, A&A, 236, 357
Conlon, E. S., Dufton, P. L., Keenan, F. P., McCausland, R. J. H., & Holmgren, D. 1992, ApJ, 400, 273

Cutri, R. M., et al. 2003, 2MASS All-Sky Catalog of Point Sources (Pasadena: IPAC)
Dorman, B., Rood, R. T., & O'Connell, R. W. 1993, ApJ, 419, 596
Edelmann, H., Heber, U., Altmann, M., Karl, C., & Lisker, T. 2005, A&A, 442, 1023
Flynn, C., Sommer-Larsen, J., & Christensen, P. R. 1994, MNRAS, 267, 77
Gilmore, G., & Reid, N. 1983, MNRAS, 202, 1025
Gratton, R. G. 1998, MNRAS, 296, 739
Gray, D. F. 1992, The Observation and Analysis of Stellar Photospheres (2nd ed.; Cambridge: Cambridge Univ. Press)
Green, R. F., Schmidt, M., & Liebert, J. 1986, ApJS, 61, 305
Harris, H. C., et al. 2003, AJ, 126, 1023
Kilkenny, D. 1995, MNRAS, 277, 920
Kilkenny, D., Heber, U., & Drilling, J. S. 1988, S. African Astron. Obs. Circ., 12, 1
Kilkenny, D., & Muller, S. 1989, S. African Astron. Obs. Circ., 13, 69
Kilkenny, D., O'Donoghue, D., & Stobie, R. S. 1991, MNRAS, 248, 664
Kinman, T., & Castelli, F. 2002, A&A, 391, 1039
Koornneef, J. 1983, A&A, 128, 84

Mitchell, K. J., Saffer, R. A., Howell, S. B., & Brown, T. M. 1998, MNRAS, 295, 225

Morales-Rueda, L., Maxted, P. F. L., Marsh, T. R., Kilkenny, D., & O'Donoghue, D. 2006, Baltic Astron., 15, 187

Noguchi, T., Maehara, H., & Kondo, M. 1980, Ann. Tokyo Astron. Obs., 18, 55

Ortiz, R. 2002, Bull. Astron. Soc. Brazil, 21, 41

Pier, J. R. 1982, AJ, 87, 1515

———. 1983, ApJS, 53, 791

Sanduleak, N. 1988, ApJS, 66, 309

Sanduleak, N., & Pesch, P. 1987, ApJS, 63, 809

Sirko, E., et al. 2004, AJ, 127, 899

Skrutskie, M. F., et al. 1997, in The Impact of Large Scale Near-IR Sky Surveys, ed. F. Garzon et al. (Dordrecht: Kluwer), 25

Sluis, A. P. N., & Arnold, R. A. 1998, MNRAS, 297, 732

Sommer-Larsen, J., & Christensen, P. R. 1986, MNRAS, 219, 537

Stetson, P. B. 1991, AJ, 102, 589

Stobie, R. S., Morgan, D. H., Bhatia, R. K., Kilkenny, D., & O'Donoghue, D. 1987, in IAU Colloq. 95, Second Conference on Faint Blue Stars, ed. A. G. D. Philip, D. S. Hayes, & J. W. Liebert (Schenectady: Davis), 493

Wilhelm, R., Beers, T. C., & Gray, R. O. 1999a, AJ, 117, 2308

Wilhelm, R., Beers, T. C., Sommer-Larsen, J., Pier, J. R., Layden, A. C., Flynn, C., Rossi, S., & Christensen, P. R. 1999b, AJ, 117, 2329

York, D. G., et al. 2000, AJ, 120, 1579